Circular Aperture Slot Antenna With Common-Mode Rejection Filter Based on Defected Ground Structures for Broad Band

Edgar Colín-Beltrán, Alonso Corona-Chávez, *Senior Member, IEEE*, Tatsuo Itoh, *Life Fellow, IEEE*, and J. Eduardo Mendoza-Torres

***Abstract*—A novel system composed of a circular aperture slot antenna and a Common-Mode (CM) noise rejection filter is presented. This antenna is differentially fed by microstrip coupled transmission lines. In order to eliminate CM noise, a notch filter based on three non-periodical defected ground structures (DGS) was implemented. The whole system achieves a fractional impedance bandwidth of about 127%. Radiation patterns in E and H planes for different frequencies were obtained for the system. Finally, measurements in the transversal plane show attenuation up to 13 dB when the system with filter was compared against one without it. Good agreement between simulated and measured results can be observed.**

***Index Terms*—Microstrip antennas, microwave filters, noise measurements.**

I. Introduction

AMONG the diversity of microwave devices, differential systems have been target of great interest. Their advantages include the ability to reject the effect of cross-talk coupling, their higher gain due to the usage of differential amplifiers and the capability of signals to travel longer distances when twisted pairs are used [1]. However, they can also guide Common-Mode (CM) currents which will contribute to the electromagnetic noise even more than Differential-Mode (DM) currents [2]. In digital applications efforts have been made in order to eliminate CM currents without affecting DM signal at high frequencies [3]–[7]. In [6] and [7], defected ground plane structures (DGS) below a pair of coupled microstrip transmission lines have been used.

On the other hand, in fields such as radioastronomy there are many applications that require very wide operational bandwidth (BW) in excess of 100% [8], [9]. These applications demand a very broad band for observation and decreased noise within those ranges. Large antenna arrays are often used to receive signals in a specific range [8]–[11] where every single element operates at the same frequency. Thus, each element can also radiate undesirable power within the operational bandwidth which can couple in the form of CM noise to adjacent antennas [2]. For broad band arrays, antennas such as Vivaldi [12] may be fed by differential signal delivered by a rat-race coupler [13]. However, by doing this, a component of CM current is inherently induced as noise, so a balun is necessary to cancel CM currents. In [14] and [15], it is shown that the effect of CM currents can be clearly observed in the cross-polarization radiation pattern. In order to detect this effect, some modifications to their original designs were made so that the balanced currents properly feed the antennas by two coaxial cables. In [16] and [17] an array of several elements was needed to observe the effect of CM radiation noise. In [18] a system made by a microstrip antenna with a BW of 10% and a CM rejection filter is reported, but as well as [16] and [17], a multilayer configuration is needed.

In this paper, a balanced system (filter-antenna) with CM noise rejection for a wide band around 127% from 2.4 to 10 GHz is presented suitable for radio astronomical observations [19]. The system was made entirely in two layers of 2D technology and it was built from two components, namely: a differentially-fed circular aperture slot antenna (CASA) and a novel filter based on DGS technology with measured BW of about 133% from 2 to 10 GHz. It will be shown that in this subsystem the CM attenuation is below -10 dB throughout the band, decreasing transversal radiation up to 13 dB near the center frequency. Moreover, unlike those prior works [14]–[18], an original form to prove the efficiency of an antenna with CM noise rejection is now proposed, where the in-phase currents are attenuated by a filter which leads to a reduction of radiation emitted by the antenna in a transversal plane. It is obtained experimentally in a straightforward way following the noise theory described in Section II.

The paper is organized as follows. Section II is about theory of CM noise. Section III describes the design procedure of the slot antenna. Its principal characteristics are described and a schematic of the novel element is presented. Simulated results of the reflection coefficient and radiation patterns are also shown. In Section IV the DGS filter is presented with its simulated and measured results. In Section V implementation of the antenna-filter system is described. Simulated and measured radiation patterns in E and H planes are presented. Section VI presents radiation patterns in a transversal plane to compare radiation produced by CM currents with filter and without it. It is evidenced that significant attenuation is achieved with the filter. Finally, conclusions are given.

Manuscript received July 20, 2012; revised November 27, 2012; accepted January 29, 2013. Date of publication February 11, 2013; date of current version May 01, 2013.

E. Colín-Beltrán, A. Corona-Chávez, and J. E. Mendoza-Torres are with the Instituto Nacional de Astrofisica, Optica y Electronica, (INAOE), San Andres Cholula, Puebla 72840, Mexico (e-mail: edgarcb@inaoep.mx).

T. Itoh is with University of California, Los Angeles, Los Angeles, CA 90095 USA (e-mail: itoh@ee.ucla.edu).

Digital Object Identifier 10.1109/TAP.2013.2246535

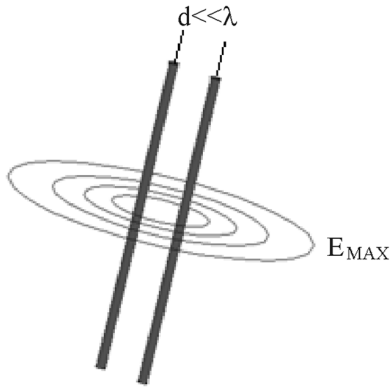

Fig. 1. Electric field lines produced by CM currents in nearby wires.

II. Common-Mode Noise Radiation in Differentially-Fed Antenna

The ubiquity of CM noise makes difficult to design electronic circuits at high frequencies [2]. Fig. 1 shows a schematic of two radiating wires where CM currents produce electric fields in an omnidirectional mode, transversal to the direction where the transmission lines are placed [2].

An electric field produced by a wire conductor can be calculated by the half-wave dipole ($\boldsymbol{L} = \lambda/2$) theory. If two wire conductors are placed close each other, the total electric field is the product of superimposing the field of each metallization. This situation can be seen as the array factor of a two element linear array, where the total electric field ($\boldsymbol{E}$) is the sum of the individual ones (1)

$$E_T = E_1 + E_2. \tag{1}$$

Equations for the magnitude of maximum emissions for DM and CM currents are given by (2) and (3)

$$|E_{Dmax}| = 1.316 \times 10^{-14} \frac{|I_D| f^2 L s}{d} \tag{2}$$

$$|E_{Cmax}| = 1.257 \times 10^{-6} \frac{|I_C| f L}{d} \tag{3}$$

where $\boldsymbol{I_D}$ and $\boldsymbol{I_C}$ are differential and common mode currents, $\boldsymbol{f}$ is frequency in Hz, $\boldsymbol{L}$ is the length of the conductors, $\mathbf{s}$ is the separation between the conductors and $\boldsymbol{d}$ is the distance where the field is measured [2].

It is worth noting that Common-Mode electric field increases linearly to the frequency. In addition, it does not depend on the separation of the conductors (although a small separation is implied) and the first term of the right side in (3) is larger than that of the differential field in (2), which indicates that the total $\boldsymbol{E}$ is dominated by CM current rather than DM current. More importantly, CM radiation covers an omnidirectional region whereas DM has a maximum within the plane of the conductors, which otherwise would be zero [2]. Then, CM currents must be avoided in systems which are used in the vicinity of other electricity conductors as in arrays of balanced antenna arrays. Based on that, the transversal plane to the transmission lines has to be tested in order to find the amount of radiation that CM current can produce around it.

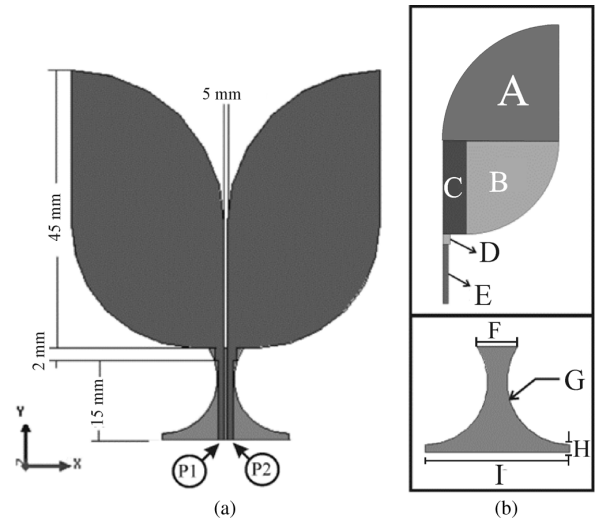

Fig. 2. (a) Diagram of CASA. (b) Detailed description of one half of top metallization (up) and ground plane (bottom).

TABLE I
Dimensions of Detailed Figures

Letter	Brief description	Dimension (mm)	Dimension (λ_G)
A	Radius of major quarter	25	0.83
B	Radius of minor quarter	20	0.66
C	Rectangle C	20 x 5	0.66 x 0.16
D	Rectangle D	2 x 1.5	0.16 x 0.05
E	Rectangle E	13 x 1	0.43 x 0.03
F	Minor base of ground plane	5.7	0.19
G	Radius of curved slot in ground plane	8.9	0.3
H	Height until curved slot of ground plane	1.1	0.37
I	Major base of ground plane	20.5	0.68

III. Circular Aperture Slot Antenna (CASA)

Tapered slot antennas (TSA) are used in applications that require a very wide operational bandwidth [20]. In this work a novel CASA is proposed. In order to maintain narrow beam in the E plane, two quarters of circles with different radii were used to build the aperture as it is shown in Fig. 2(b), ($\mathbf{A}$ and $\mathbf{B}$). The rectangle labeled with $\mathbf{C}$ is used to fill the space due to the difference of radii. On the other hand, to obtain differential current between ports $\mathbf{P1}$ and $\mathbf{P2}$, the width and separation of microstrip coupled lines (rectangle $\mathbf{E}$) were calculated to obtain 50 Ω for odd-mode propagation. The optimization of lines required a rectangle $\mathbf{D}$ on each line. The ground plane was modified to a curved profile with 8.9 mm of radius on each side (letter $\mathbf{G}$). All the optimizations were done in a full-wave simulator [21]. The final design is shown in Fig. 2 and dimensions are detailed in Table I. The last column describes dimensions referred to $\lambda_G = 30$ mm at 6 GHz in Rogers Duroid 4003C with a relative permittivity of 3.55 and thickness of 0.813 mm.

In order to obtain the reflection coefficient ($\boldsymbol{S_{11dd}}$) for DM, (4) is utilized [11] as

$$S_{11dd} = \frac{1}{2}(S_{11} - S_{12} - S_{21} + S_{22}) \tag{4}$$

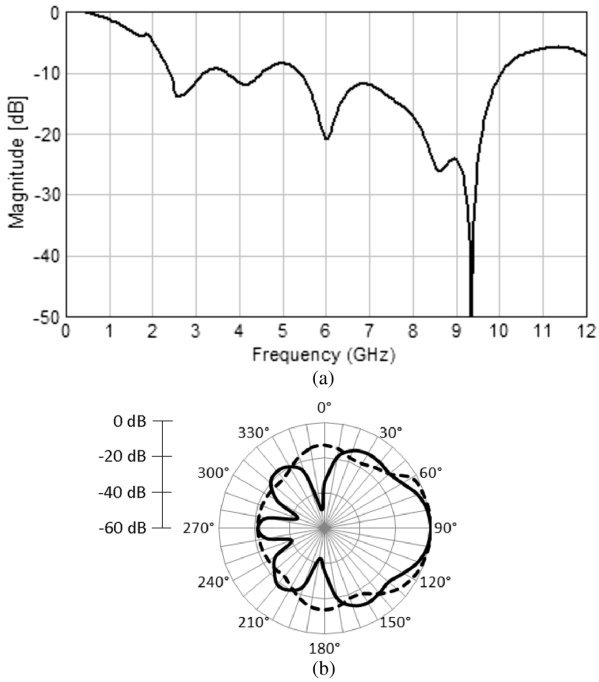

Fig. 3. Simulated results of CASA. (a) Reflection coefficient, (b) radiation patterns at center frequency: E-plane: continuous line, H-plane: dashed line.

where the S-parameters are extracted of the two-port network matrix obtained from ports $\mathbf{P1}$ and $\mathbf{P2}$. Simulated results are presented in Fig. 3(a). From here it is seen that the operational BW beneath -10 dB is about 127% from 2.4 to 10 GHz. There are two peaks above this limit at 3.5 and 5 GHz. These shortcomings will be removed when the filter is added in Section V. A remarkable advantage is the high level of symmetry in radiation patterns on end-fire direction because of the differential currents that are placed on the same plane, unlike antipodal version of a Vivaldi, [22]. Moreover balanced currents give lower cross-polarization levels than the antipodal version [23].

The symmetry along maximum radiation (90°) can be clearly appreciated in the results of simulation patterns on Fig. 3(b). As it can be deduced from [20], E plane has a narrow beamwidth less than 60° at 3 dB, whereas the H plane pattern is wider due to relative short length in the Y axis of the antenna.

IV. DGS Filter Design and Implementation

In this section the balanced filter concept is explained. In a microstrip coupler transmission line, DM signal is propagated by the odd-mode between top lines; therefore low return current is flowing through the ground plane. On the other hand, the return CM current related to the even-mode is transported principally by the ground plane, so a DGS [24] will have a significant effect on the CM signal ([6], [7] and [24]). Our filter is shown in Fig. 4. Unlike [7] and [24] the structures used here have hourglass form as their central slot is curved. Those gaps were built by the approaching of two ellipses. These curved slots increase the smoothness of the change in capacitance and the BW can be extended beyond 100% as opposed as 87% and 53%

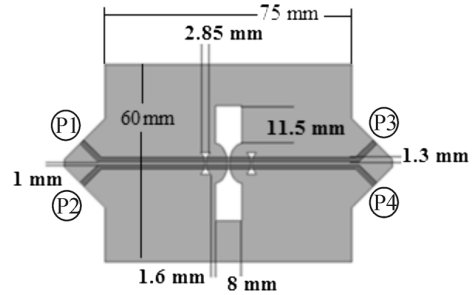

Fig. 4. Filter with dimensions. Lighter gray is ground plane, dark one is top metallization. Each port is indicated with its number.

obtained in [6] and [7], respectively. The narrowest spaces in the middle of the slots are about 0.45 and 0.55 mm for side and central shape, respectively. Another important difference from the previous three-DGS works is that in our filter the shapes are not periodic. Side DGSs have a height of 6.5 mm meanwhile central shape has 35 mm; this latter structure is larger because the lower rejection frequency is determined by it. The dimensions and spaces between the three slots were optimized using full-wave simulator [21].

The behavior of these filters is described principally by the insertion loss for DM ($\boldsymbol{S_{21dd}}$) extracted form (5) and insertion loss for CM ($\boldsymbol{S_{21cc}}$) obtained from (6) ([6] and [7]). But we also calculate the reflection coefficient for DM ($\boldsymbol{S_{11dd}}$) from (4) given in Section III, so that the system can be fully characterized [25]

$$S_{21dd} = \frac{1}{2}(S_{31} - S_{32} - S_{41} + S_{42}) \tag{5}$$

$$S_{21cc} = \frac{1}{2}(S_{31} + S_{32} + S_{41} + S_{42}). \tag{6}$$

Note that S-parameters of the right side in (4) are extracted from the two-port network matrix obtained from ports 1 and 2, as in previous section. $\boldsymbol{S_{31}}$ and $\boldsymbol{S_{32}}$ are the insertion losses from port 1 and port 2 to port 3, meanwhile $\boldsymbol{S_{41}}$ and $\boldsymbol{S_{42}}$ are the insertion losses from port 1 and 2 to port 4. The ports are indicated with letter $\mathbf{P}$ and their corresponding number in Fig. 4.

Implementation of the filter was made in the substrate same as the simulated CASA in Section III. As it can be seen on Figs. 5 and 6, simulated and measured results, obtained from (4)to (6), are in reasonable agreement. A BW of about 133% (2 to 10 GHz) is achieved for a DM insertion loss less than 3 dB and for CM insertion and DM return losses more than 10 dB. A small ripple occurs at higher frequencies close to 10 GHz, which is thought to be due to the discontinuity presented between each SMA connector and microstrip transmission line.

It is worth noting that simulated parameters of the filter reported in [7] were extracted and included in the Figs. 5 and 6. As it can be seen in Fig. 5, filter proposed in [7] covers only about 63% (2.9 GHz to 5.6 GHz) for CM rejection larger than 10 dB. In addition in Fig. 6; the DM reflection coefficient of [7] is limited until 7 GHz below -10 dB.

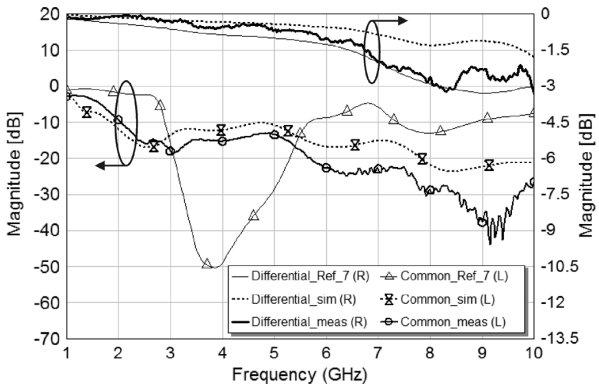

Fig. 5. Simulation and measured insertion losses of the filter for Common- and Differential-Modes. The simulated DGS filter response from reference [7] is included for comparison.

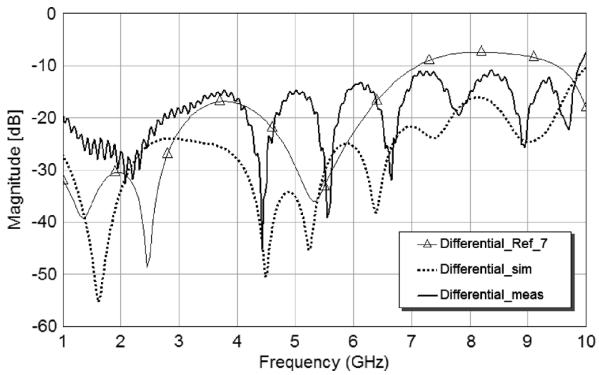

Fig. 6. Simulation and measured reflection coefficients of filter for Differential-Mode. The simulated DGS filter response from reference [7] is included for comparison.

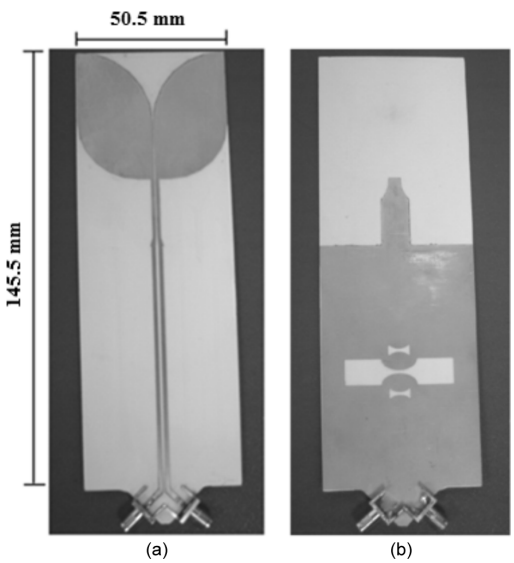

Fig. 7. Photograph of the system (Filter-Antenna). (a) Top view, (b) Bottom view.

V. Attachment of CM-Reject Filter and CASA

A. Filter Matching Characteristics

An image of the antenna-filter system is shown in Fig. 7. Implementation of the antenna with the filter and a reference board without it were made in the same substrate as the DGS-filter, the complete subsystem fits on a rectangle of 145.5 mm × 50.5 mm.

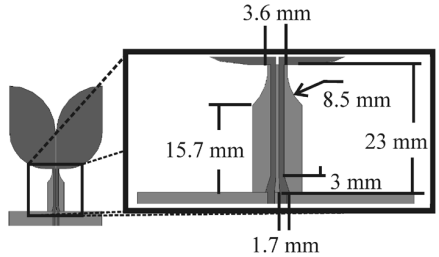

Fig. 8. Matching transition between filter and CASA. Lighter gray is ground plane, dark one is top metallization.

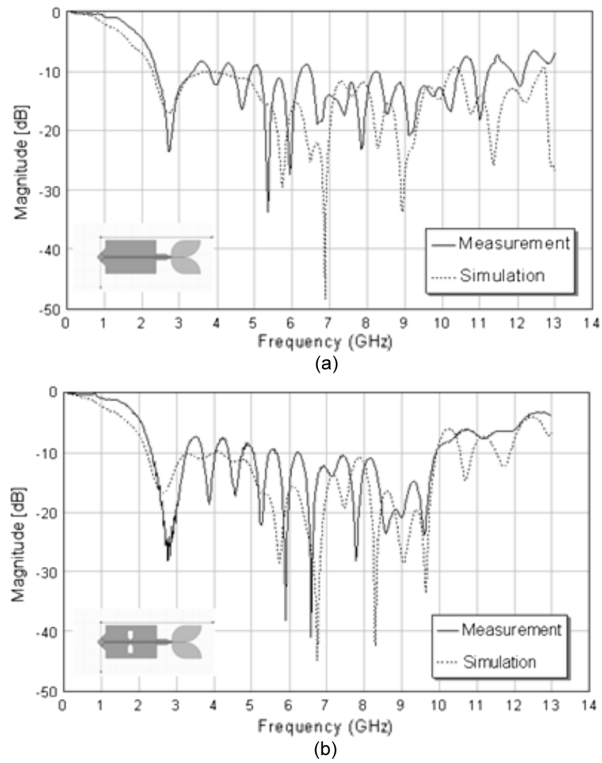

Fig. 9. Reflection coefficients for the CASA: (a) Without filter, (b) With filter. As it can be seen, differential signal is not affected by the filter along the band.

The filter was included with no other modifications but the elimination of tapered feeds marked as **P3** and **P4** in Fig. 4, so that the antenna can be connected at that terminations. Since the dimensions of transmission lines in the antenna are different to those of the filter, a combination of step-tapered microstrip line was used to match them (see Fig. 8). Moreover, the original ground plane of antenna were slightly modified, **F** and **I** (Fig. 2) were decreased from 5.7 to 3.6 mm and from 20.5 to 9 mm, respectively. The microstrip couplings and ground plane modifications were optimized in [21].

Measured and simulated results of differential reflection coefficient for systems with filter and without filter are presented in Fig. 9(a) and (b). A two-port single-ended matrix was obtained from each system, and $\boldsymbol{S_{11dd}}$ was extracted from (4). Return losses for simulations are always greater than 10 dB and for measurements greater than 8.35 dB within a BW of about to 127%, for both systems.

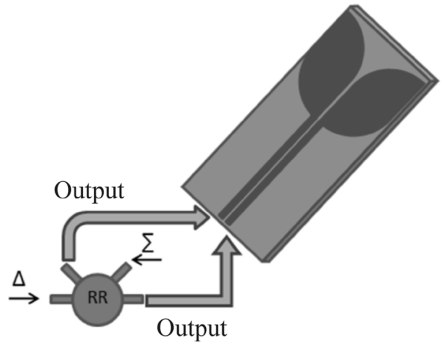

Fig. 10. Schematic of the union of rat-race coupler to system. Σ-input gives two signals with 0° phase shift. Δ-input gives two signals with 180° phase shift.

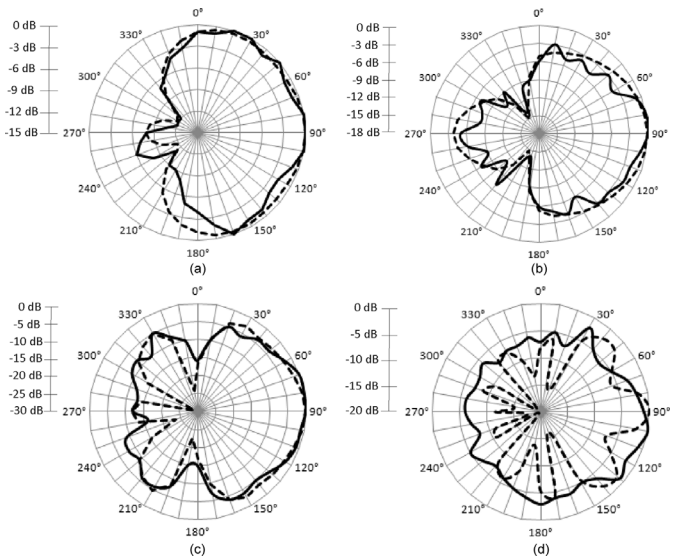

Fig. 11. Radiation patterns with filter in E plane at (a) 2.9 GHz, (b) 4.3 GHz, (c) 6 GHz and (d) 10 GHz. (Simulation: dashed line; measurement: continuous line).

B. Radiation Patterns

In order to feed the antenna, the system needs to have a phase shifting of 180° between the coupled transmission lines. For this reason a rat-race coupler (RRC) was used as observed in Fig. 10. This coupler has four ports and it was used as a power divider. Port Δ was fed to obtain the split of one voltage at the output ports, with 180° shifting between them. Port Σ was loaded with 50 Ω [26]. Three different RRC's based on [13] were implemented to cover the whole BW of interest (as each coupler's BW is only about 50%). The first coupler covers from 2.5 GHz to 4.5 GHz, the second from 4.8 GHz to 7.3 GHz and the third one from 6.5 GHz to 10.8 GHz. The same substrate of the previous components was used.

Radiation patterns in E and H planes were obtained at four different frequencies (2.9 GHz, 4.3 GHz, 6 GHz and 10 GHz) and they can be observed in Figs. 11 and 12, respectively. Simulated and measured results are in good agreement.

The end-fire gain for DM is shown in Fig. 13. As it can be seen, a maximum of 9 dBi is obtained at 4 GHz and along the entire BW it is about 5 dBi, which is in line with this type of antennas [20].

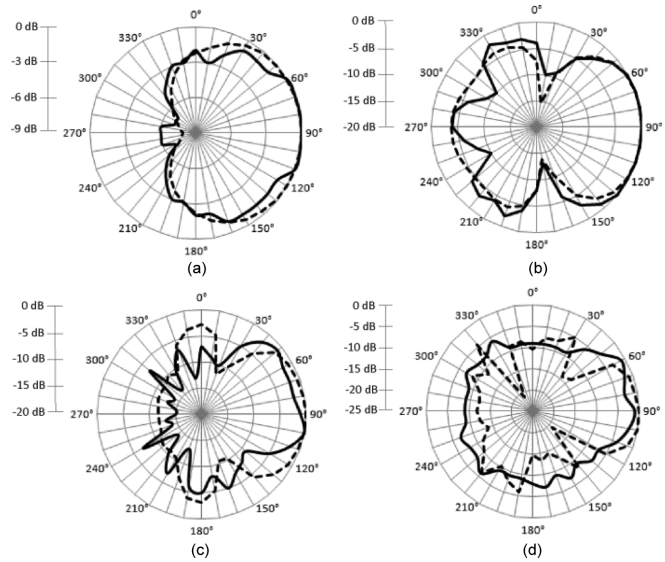

Fig. 12. Radiation patterns with filter in H plane at (a) 2.9 GHz, (b) 4.3 GHz, (c) 6 GHz and (d) 10 GHz. (Simulation: dashed line; measurement: continuous line).

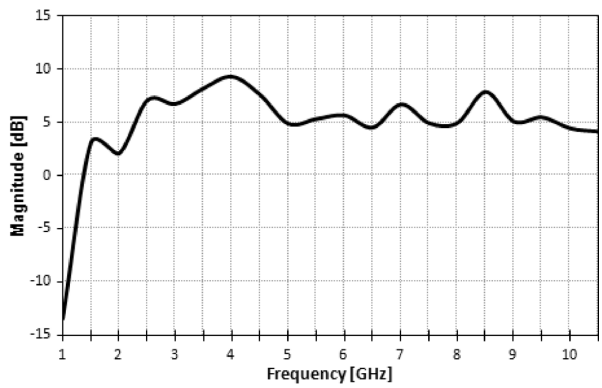

Fig. 13. Measurement of gain along the frequency for CASA with filter.

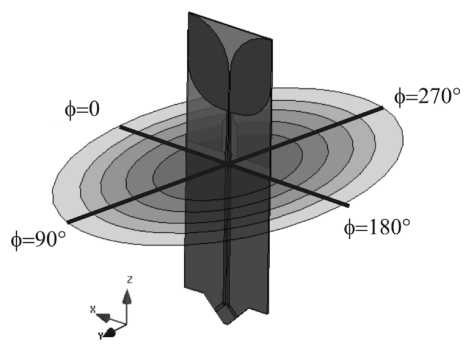

Fig. 14. Radiation pattern in transversal direction to CM currents.

VI. Common Mode Noise Radiation

In order to quantify the transversal emission of CM fields as shown in Section II, the radiation pattern in the transversal direction, as depicted in Fig. 14, was measured. Using the setup of Fig. 10, two in-phase currents derived from the Σ-port of the rat-race couplers were input to the systems with and without filter (a load was connected to the Δ-port).

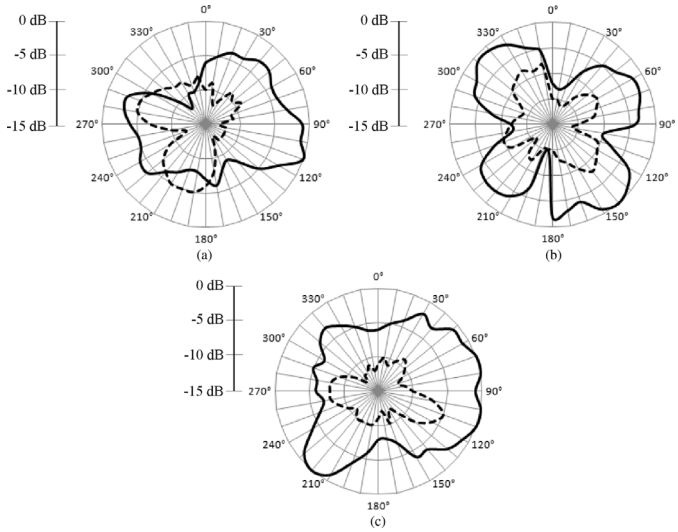

Fig. 15. Radiation pattern of comparisons with and without filter at (a) 3 GHz, (b) 5.5 GHz and (c) 7 GHz. (Filter: dashed line; without filter: continuous line).

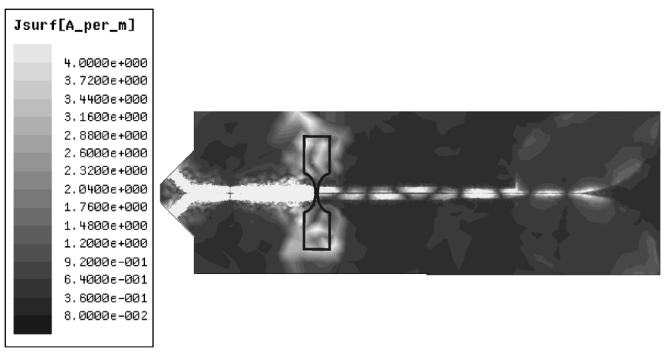

Fig. 16. CM-surface current density for CASA-filter system at 3 GHz. The DGS resonance reaches a maximum of current at its borders which produce radiation.

The measured radiation patterns with and without filter at three different frequencies within the band of interest (3 GHz, 5.5 GHz and 7 GHz) are shown in Fig. 15. It is clearly seen that transversal radiation is highly suppressed by the addition of the filter. This suppression is in order of 13 dB at 180° and 230° for 5.5 GHz, where maximum cancellation is achieved. For 7 GHz suppression reaches a maximum of 12 dB at 70°, and for 3 GHz the highest attenuation is 12 dB from 90° to 110°. Nonetheless, the level of radiation with the filter is higher than that without it between 170° to 210° and from 300° to 350°. This is attributed to a resonant effect of the largest DGS structure, therefore increasing transversal radiation, as shown in Fig. 16.

VII. Conclusion

A new CASA with broadband CM noise rejection filter is proposed in this paper. The system includes a CASA and a novel filter based on three non-periodical DGS, on a 2D technology. Simulated and measured results of the system were obtained with accuracy within the broad BW of about 127% from 2.4 to 10 GHz. Several radiation patterns for E and H planes were taken showing good agreement with simulated results. Finally, the radiation due to CM currents was obtained by an innovative measurement of the pattern in the transversal plane, which shows a maximum attenuation of 13 dB for the system with filter. This element can be attractive to use in a dense array of antennas given its low adjacent radiation and broad band of operation.

References

[1] E. Bogatin, *Signal Integrity-Simplified*, ser. Modern Semiconductor Design Series. Englewood Cliffs, NJ, USA: Prentice Hall, 2004.
[2] C. R. Paul, *Introduction to Electromagnetic Compatibility*, 2nd ed. Hoboken, NJ, USA: Wiley, 2006.
[3] C.-H. Wu, C.-H. Wang, and C.-H. Chen, "Balanced coupled-resonator bandpass filters using multisection resonators for common-mode suppression and stopband extension," *IEEE Trans. Microw. Theory Tech.*, vol. 55, no. 8, pp. 1756–1763, Aug. 2007.
[4] C.-H. Tsai and T.-L. Wu, "A broadband and miniaturized common-mode filter for gigahertz differential signals based on negative-permittivity metamaterials," *IEEE Trans. Microw. Theory Tech.*, vol. 58, no. 1, pp. 195–202, Jan. 2010.
[5] C.-H. Wu, C.-H. Wang, and C.-H. Chen, "Stopband-extended balanced bandpass filter using coupled stepped-impedance resonators," *IEEE Trans. Microw. Theory Tech.*, vol. 17, no. 7, pp. 507–509, Jul. 2007.
[6] S.-J. Wu, C.-H. Tsai, T.-L. Wu, and T. Itoh, "A novel wideband common-mode suppression filter for gigahertz differential signals using coupled patterned ground structure," *IEEE Trans. Microw. Theory Tech.*, vol. 57, no. 4, Apr. 2009.
[7] W.-T. Liu, C.-H. Tsai, T.-W. Han, and T.-L. Wu, "An embedded common-mode suppression filter for GHz differential signals using periodic defected ground plane," *IEEE Microw. Wireless Comp. Lett.*, vol. 18, no. 4, pp. 248–250, Apr. 2008.
[8] Special Astrophysics Observatory, Radiotelescope RATAN-600 [Online]. Available: http://www.sao.ru/ratan/
[9] S. Claude and J. di Francesco, High Frequency Receiver Development for Astronomy [Online]. Available: http://www.casca.ca/lrp2010/Docs/LRPReports/mm.inst.pdf
[10] J. G. Bij de Vaate *et al.*, "Low cost low noise phased-array feeding systems for SKA pathfinders," presented at the 13th Int. Symp. On Antenna Technology and Applied Electromagnetics and the Canadian Radio Sciences Meeting, Feb. 2009.
[11] M. Arts, R. Maaskant, E. L. Acedo, and J. G. Bij de Vaate, Broadband Differentially Fed Tapered Slot Antenna for Radio Astronomy Applications [Online]. Available: http://www.skads-eu.org/PDF/EuCAP2009.pdf
[12] P. J. Gibson, "The Vivaldi aerial," presented at the 9th Eur. Microwave Conf., 1979.
[13] M. Caillet, "A compact wide-band rat-race coupler hybrid using microstrip lines," *IEEE Microw. Wireless Comp. Lett.*, vol. 19, no. 4, pp. 191–193, Apr. 2009.
[14] R. Bourtoutian, C. Delaveaud, and S. Toutain, "Differential antenna design and characterization," presented at the 3rd. Conf. on Antenas and Propagation, 2009.
[15] A. V. Vorobyov, J. H. Zijderfeld, A. G. Yarovoy, and L. P. Ligthart, "Impact common mode currents on miniaturized UWB antenna performance," presented at the Eur. Conf. on Wireless Technology, 2005.
[16] D. Cavallo, A. Neto, and G. Gerini, "PCB slot based transformers to avoid common-mode resonances in connected arrays of dipoles," *IEEE Trans. Antennas Propag.*, vol. 58, no. 8, pp. 2767–2771, Aug. 2010.
[17] L. Cifola, D. Cavallo, G. Gerini, S. Savoia, A. Morini, and G. Venanzoni, "Common-mode rejection in a connected array of dipoles with inherent frequency selectivity properties," presented at the 6th Eur. Conf. on Antennas and Propagation (EUCAP), Mar. 2012.
[18] H.-C. Chen and T.-L. Wu, "Suppression of RF interference using balanced filter in communication system," in *Proc. IEEE Int. Symp. on Electromagnetic Compatibility (EMC)*, 2011, pp. 564–568.
[19] Y. Y. Kovalev, L. I. Gurvits, and G. Gorshkov, "Violently variable blazer 0524+034 as seen by EVN, VLBA and VSOP," in *Proc. 10th Anniversary of the VLBA, ASP Conf.*, 2005, vol. 340.
[20] C. A. Balanis, *Antenna Theory: Analysis and Design*, 2nd ed. New York, New York, USA: Wiley, 1997.
[21] Ansoft Corporation, HFSSv.12.
[22] E. Gazit, "Improved design of the Vivaldi antenna," *Inst. Elect. Eng. Proc.-H, Microw., Antennas Propag.*, vol. 135, no. 2, pp. 89–92, Apr. 1998.
[23] J. D. S. Langley, "Balance antipodal Vivaldi antenna for wide bandwidth phased arrays," *IEE Proc. Microw. Antenas Propag.*, vol. 143, no. 2, pp. 97–102, Apr. 1996.

[24] D. Ahn, J.-S. Park, C.-S. Kim, J. Kim, Y. Qian, and T. Itoh, "A design of the low-pass filter using the novel microstrip defected ground structure," *IEEE Trans. Microw. Theory Tech.*, vol. 49, no. 1, pp. 86–93, Jan. 2001.
[25] W. Fan, A. C. W. Lu, L. L. Wai, and B. K. Lok, Mixed-Mode S-Parameter Characterization of Differential Structures [Online]. Available: http://www.simtech.a-star.edu.sg/Research/TechnicalReports/TR04JT03.pdf
[26] D. M. Pozar, *Microwave Engineering*, 3rd ed. Hoboken, NJ, USA: Wiley, 2005.

Edgar Colín-Beltrán was born in Toluca, Mexico, in 1981. He received the B.Sc. degree from the Universidad Autonoma del Estado de Mexico (UAEM), Mexico, in 2004 and the M.Sc. degree from the Instituto Nacional de Astrofisica, Optica y Electronica (INAOE), Tonantzintla, Puebla, Mexico, in 2007, where he is currently working towards the Ph.D. degree.

He was collaborator with the Electrical Engineering Department, University of California at Los Angeles (UCLA) in 2011. His research interest includes UWB microwave antennas and phased array antennas for radioastronomy.

Alonso Corona-Chávez (S'00–A'01–M'02–SM'09) received the B.Sc. degree from the Tecnológico de Monterrey (ITESM), México, in 1997 and the Ph.D. degree from the University of Birmingham, Edgbaston, Birmingham, U.K., in 2001.

From 2001 to 2004, he was a Microwave Engineer with Cryosystems Ltd. During this time, he was also an Honorary Research Fellow with the School of Electrical Engineering, University of Birmingham. In 2004, he joined the Instituto Nacional de Astrofisica, Óptica y Electrónica (INAOE), Tonantzintla, Puebla, México, where he is currently a Professor of electronics. He is the Head of the Emerging Microwave Technologies Group (EMT), INAOE. His current interests include microwave applications of HTS, RF, and microwave devices for communications and radio astronomy.

Prof. Corona-Chávez was the recipient of a Fulbright Fellowship to carry out research with the Electrical Engineering Department, University of California at Los Angeles (UCLA) in April 2009.

Tatsuo Itoh (S'69–M'69–SM'74–F'82–LF'06) received the Ph.D. Degree in electrical engineering from the University of Illinois, Urbana, IL, USA, in 1969.

After working for University of Illinois, SRI and University of Kentucky, he joined the faculty at The University of Texas at Austin, Austin, TX, USA, in 1978, where he became a Professor of Electrical Engineering in 1981. In September 1983, he was selected to hold the Hayden Head Centennial Professorship of Engineering at The University of Texas. In January 1991, he joined the University of California, Los Angeles, CA, USA, as Professor of Electrical Engineering and holder of the TRW Endowed Chair in Microwave and Millimeter Wave Electronics (currently Northrop Grumman Endowed Chair). He has 400 journal publications, 820 refereed conference presentations and has written 48 books/book chapters in the area of microwaves, millimeter-waves, antennas and numerical electromagnetics. He has supervised up to 73 Ph.D. students.

Dr. Itoh received several awards, including IEEE Third Millennium Medal in 2000, and IEEE MTT Distinguished Educator Award in 2000. He was elected to a member of National Academy of Engineering in 2003. In 2011, he received Microwave Career Award from IEEE MTT Society. He is a member of the Institute of Electronics and Communication Engineers of Japan, and Commissions B and D of USNC/URSI. He served as the Editor of IEEE TRANSACTIONS ON MICROWAVE THEORY AND TECHNIQUES for 1983–1985. He was President of the IEEE Microwave Theory and Techniques Society in 1990. He was the Editor-in-Chief of IEEE MICROWAVE AND GUIDED WAVE LETTERS from 1991 through 1994. He was elected as an Honorary Life Member of MTT Society in 1994. He was the Chairman of Commission D of International URSI for 1993–1996. He serves on advisory boards and committees of a number of organizations. He served as Distinguished Microwave Lecturer on Microwave Applications of Metamaterial Structures of IEEE MTT-S for 2004–2006.

J. Eduardo Mendoza-Torres received the B.Sc. degree from the Faculty of Physics and Mathematics, Universidad Autonoma de Puebla (BUAP), Puebla, Mexico and the Ph.D. degree in astrophysics and radioastronomy from the Special Astrophysical Observatory, Russian Academy of Sciences, Russia.

From 1986 to 1987, he was a Senior Teacher at the Faculty of Physics and Mathematics, BUAP, and from 1993 to 2012 he was a Senior Researcher in the Department of Astrophysics, Instituto Nacional de Astrofisica Optica y Electronica (INAOE).

He is the author and coauthor of more than 30 refereed scientific publications, PI of the project of site testing for the Large Millimeter Telescope (GTM/LMT), PI of the project of reinstalling a 5 m dish radio telescope and responsible of the organization of the National Astronomy Olympiad at Mexico. His research interest includes instrumentation on radioastronomy applied at solar activity and galactic masers.